The ENSO Events in the Tropical Pacific and Dipole Events in the Indian Ocean*

CHAO Jiping[1,2] (巢纪平), CHAO Qingchen[3](巢清尘), and LIU Lin[2,4](刘　琳)

1 *National Marine Environment Forecast Center, Beijing* 100081

2 *The First Institute of Oceanography, SOA, Qingdao* 266061

3 *National Climate Center, Beijing* 100081

4 *Ocean University of Qingdao，Qingdao* 266003

(Received April 30, 2006)

ABSTRACT

A depth map (close to that of the thermocline as defined by 20°C) of climatically maximum sea-temperature anomaly was created at the subsurface of the tropical Pacific and Indian Ocean, based on which the evolving sea-temperature anomaly at this depth map from 1960 to 2000 was statistically analyzed. It is noted that the evolving sea temperature anomaly at this depth map can be better analyzed than the evolving sea surface one. For example, during the ENSO event in the tropical Pacific, the sea-temperature anomaly signals travel counter-clockwise within the range of 10°S-10°N, and while moving, the signals change in intensity or even type. If Dipole is used in the tropical Indian Ocean for analyzing the depth map of maximum sea-temperature anomaly, the sea-temperature anomalies of the eastern and western Indian Oceans would be negatively correlated in statistical sense (Dipole in real physical sense), which is unlike the sea surface temperature anomaly based analysis which demonstrates that the inter-annual positive and negative changes only occur on the gradients of the western and eastern temperature anomalies. Further analysis shows that the development of ENSO and Dipole has a time lag features statistically, with the sea-temperature anomaly in the eastern equatorial Pacific changing earlier (by three months or so). And the linkage between these two changes is a pair of coupled evolving Walker circulations that move reversely in the equatorial Pacific and Indian Oceans.

Key words: depth map of maximum sea-temperature anomaly, ENSO, Dipole, coupled evolving of Walker circulations

1. Introduction

Since Bjerknes (1966, 1969) noted in the 1960s that El Niño in the tropical Pacific and the southern oscillation in the atmosphere are actually an interconnected and interacting large scale sea-air event (called ENSO afterwards), the ENSO study has been given a lot of attention by meteorologists and oceanographers. It is generally believed that ENSO is one of the important signals that cause inter-annual global climate anomalies. In the analysis of ENSO development, the sea surface temperature anomaly (SSTA) is normally used to represent the changing ocean, and 850-hPa zonal anomaly wind represents the changing atmosphere. Using these two indicators, Rasmusson and Carpenter (1982) analyzed what the ocean and atmosphere of various phases looked like in the process of ENSO development. However, it was observed in the China-US experiment on sea-air interaction in the western Pacific that the warm sea temperature anomaly in the 1986/87 ENSO occurred first at the 80-115-m subsurface level between 147°E and 175°E (near the thermocline)(Wang et al., 1990). This observation indicates that not only the western Pacific plays a very important role in the development of El Niño (e.g., the 1982/83 positive SSTA appeared first in the equatorial western Pacific), but also the strong indicative signals of sea temperature might be firstly found at the subsurface level. Such an analysis of the relations between the development of 1997/98 El Niño and the subsurface sea temperature anomaly in the western Pacific was ever made by Li and Mu (1999).

On the other hand, Saji et al. (1999) noted that the sea surface temperature anomaly across the west-east gradient in the tropical Indian Ocean featured an inter-annual negative and positive alternation, a

*Supported by the National Natural Science Fundation of China under Grand Nos.40176002 and 40231012.

phenomenon of Dipole as they called. According to the physical definition of Dipole, however, the sea-temperature anomalies of the western and eastern Indian Ocean should look opposite in terms of symbol. Except for 1994 and 1997/98 when the symbols were opposite, such representation was rarely found for other years. This inconsistency made us explore another perspective for a renewed analysis.

2. Depth map of maximum sea-temperature anomaly and its application

In fact, it is reasonable to represent the subsurface level with the thermocline. However, if 20°C is set as a reference temperature to determine the depth of thermocline, the temperature in the cold tongue zone of the eastern equatorial Pacific is usually below 20°C, making the analysis process difficult. Moreover, the reference temperature for thermocline in the Indian Ocean is not yet agreed upon. In this context, an idea is proposed by Chao et al. (2001): creating a maximum subsurface temperature anomaly (MSTA), the depth of which is used to replace that of thermocline. The MSTA is created in this way: collecting the maximum temperature anomaly at each point under the surface (symbols not counted in), averaging the depth of all the maximums climatically and obtaining depth map, which would be the depth map of maximum sea-temperature anomaly. Meanwhile, the depth distribution of MSTA and toroidal of thermocline depth map with 20°C set as reference are comprised (Chao et al., 2003b), and they are similar.

In the following analysis, the sea subsurface temperature anomaly on the MSTA depth map will be used to replace the commonly used SSTA. The physical justification for such a replacement is that the effect by atmosphere to sea on the inter-annual scale is met primarily by the convergence, divergence or rotation of low wind stress interfering with the thermocline depth, the change of which could be indicated, to some extent, by the changing temperature on the climatic thermocline. For example, when the thermocline is shallower (deeper), the sea temperature on the climatic thermocline is cooler (warmer). On the other hand, the sea surface temperature is subject to the sensible heat, latent heat, precipitation, and evaporation in addition to the wind stress so that it changes in an elusive and feeble manner and with a lot of noise for a given temporal scale.

As an example, we can analyze how the sea temperature anomaly from 1968 to 2000 evolved on the MSTA. Figure 1 is a new figure given after the nine months signals sliding and averaging by Chao et al.'s (2003b) Fig.2.

Figure 1 clearly shows that when a warm (cool) sea temperature signal is spreading along the equator from the western Pacific warm pool eastward to the eastern Pacific and then up northward, there would be a cool (warm) sea temperature anomaly signal occurring near 10°N (normally 8°-14°N) and spreading from the eastern Pacific to the western Pacific and southward to the warm pool near the equator. Thus, the cool and warm sea temperature anomaly signals spread in different latitudes, leading to the alternation of cool and warm phases in an indicated longitude in the equator, namely an ENSO cycle. Generally in the Southern Hemisphere there is also a similar cycle for the sea temperature anomaly but not as obvious as that in the Northern Hemisphere, which is probably because of the greater depth of the extreme depth map of sea temperature anomaly to the south of equator, where the sea temperature anomaly is not strong enough for an analysis or is susceptible to disturbance.

It is impossible to make an analysis, using SSTA, of this regular pattern of sea temperature signals spreading on the MSTA depth map.

3. The sea air interaction event in the tropical Pacific Ocean (ENSO)

From Fig.1, we can see that in many cases, at a time when the equatorial eastern Pacific registers a warm (cool) temperature anomaly, the western Pacific warm pool registers a cool (warm) temperature anomaly. Figure 2 shows the curves reflecting the inter-annual changes of the western (10°N-4°S, 130°-155°E) and eastern (4°N-4°S, 90°-150°W) Pacific sea temperature anomalies on the MSTA depth map respectively (data taken from the Scripps Oceanography Institute), from which an inverse correlation can be

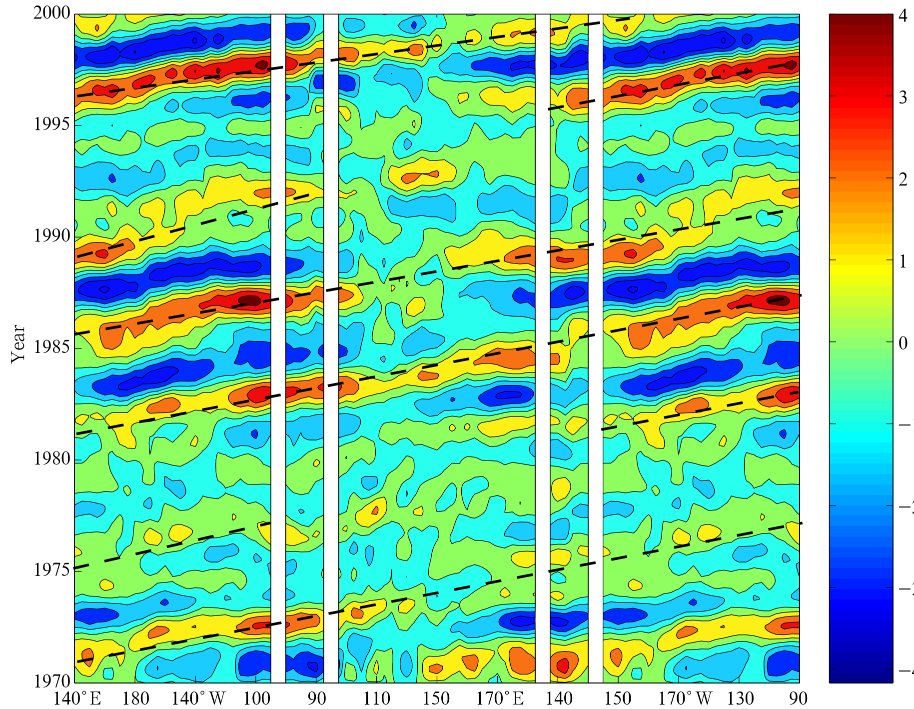

Fig.1. The evolving of sea-temperature anomaly on the MSTA. The first segment of x-axis (abscissa) represents the leg from the West Pacific (140°E) to East Pacific (115°W) along the equator; the second one from equator to 10°N along 115°W (no latitude degree indicated due to narrow space); the third from 115°W back to 140°E along 10°N; the fourth from 10°N back to equator along 140°E (no latitude degree indicated due to narrow space); and the fifth is the same as the first.

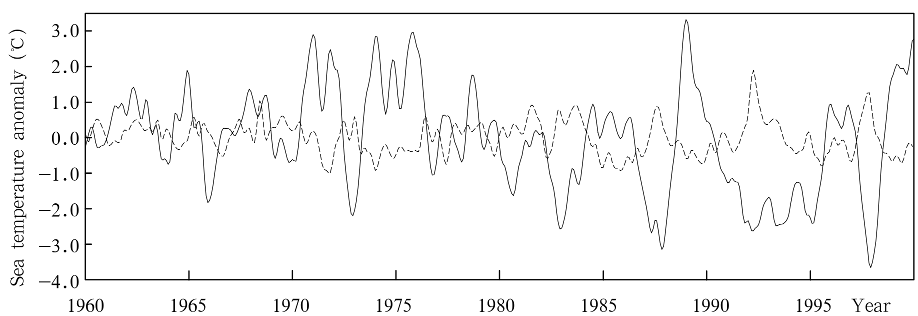

Fig.2. The inter-annual changes of the sea-temperature anomaly in the western (10°N-4°S, 130°-155°E; solid line) and eastern (4°N-4°S, 90°-150°W; dashed line) Pacific Ocean.

seen with a coefficient of -0.43 (the maximum one appearing at a time when the eastern Pacific sea temperature anomaly occurs two months earlier with a factor of -0.45). Clearly, the eastern and western Pacific sea temperature anomalies on the MSTA depth map are distributed in the form of dual poles (Dipole).

Figure 3a shows the curve reflecting the sea temperature anomaly on the MSTA depth map in the same indicated western Pacific zone as above and the curve reflecting the inter-annual change of the deep anomaly on the MSTA depth map in the corresponding zone. The two curves are of a positive correlation with a coefficient of 0.31. It can be seen that the changing sea temperature anomaly on the MSTA depth map reflects the changing depth of the thermocline. Figure 3b shows the curves reflecting the inter-annual changes of the 850-hPa zonal wind anomaly in the central Pacific (10°N-10°S, 180°-145°W) and the

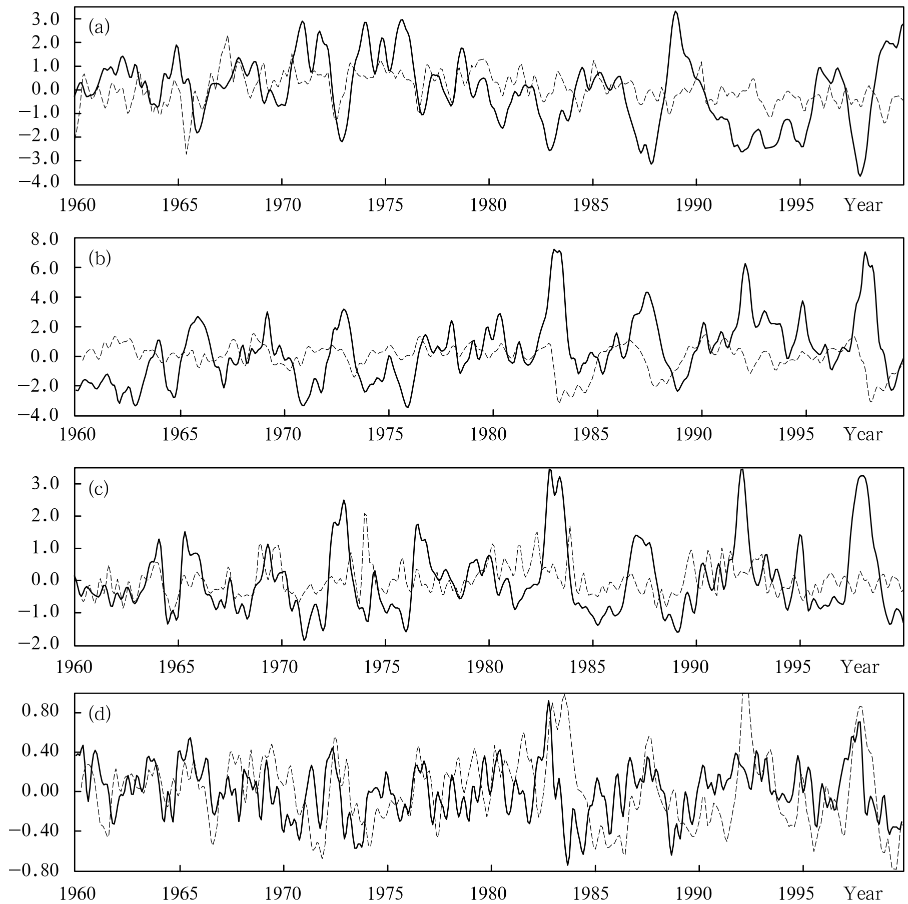

Fig.3. The inter-annual changes of subsurface sea-temperature anomaly (solid line) and the deep anomaly distribution (dashed line) on the MSTA of the western (a) and the eastern (c) Pacific Ocean; the inter-annual changes of 850-hPa zonal wind anomaly (solid line) in the central (b) and the eastern (d) Pacific Ocean and sea-temperature anomaly (dashed line) on the MSTA of the western (b) and the eastern (d) Pacific Ocean.

sea subsurface temperature anomaly in the indicated western Pacific (zonal wind earlier by three months), and they are of an inverse correlation with a coefficient of -0.51. Figure 3c show that of the eastern Pacific, where the correlation coefficient between sea temperature anomaly and changing MSTA depth is 0.28 and between sea temperature anomaly and zonal wind (earlier by four months) is a positive 0.41 (Fig.3d). These figures show that the sea temperature anomaly on the MSTA depth map can clearly outline an ENSO event.

In the figures, the zonal wind is assumed an earlier month, when the correlation coefficient registers the highest value, indicating that this phase of sea-air interaction is dominated by atmosphere. The process of how ocean interacts with atmosphere will be analyzed in a separate paper.

4. The sea-air interaction event in the tropical Indian Ocean (Dipole)

For the tropical Indian Ocean, the Dipole Index (DMI) put forward by Saji et al. (1999) actually reflects the inter-annual changes of the western and eastern Indian Ocean gradient sea surface temperature anomalies. In quite a number of cases, the western (10°N-10°S, 50°-70°E) and eastern (10°N-10°S, 90°-110°E) Indian Ocean sea temperature anomalies share the same symbols but differ in intensity. As noted by Chao et al. (2003a), if the analysis is made under the context of the Indian Ocean MSTA depth map, the inter-annual changes of the western and eastern Indian Ocean sea temperature anomalies are shown in Fig.4, which is of an inverse correlation with a coefficient of -0.38.

Figure 5a shows the inter-annual change of the above mentioned western Indian Ocean sea temperature anomaly and the inter-annual change of the corresponding MSTA depth map, the correlation coefficient of 0.32. This equally indicates that it is the same case with the Indian Ocean, namely, the changing temperature on the MSTA depth map is the reflection of the changing depth map. Figure 5b also gives curves reflecting the changing central Indian Ocean (4°N-10°S, 60°-80°E) zonal wind and the western Indian Ocean subsurface temperature anomaly. The temperature anomaly and zonal wind anomaly are of an inverse correlation with a coefficient of -0.34. Figure 5c shows the eastern Indian Ocean, where the correlation coefficient between the sea temperature anomaly and

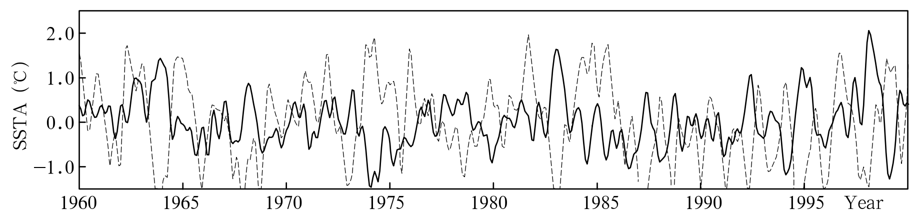

Fig.4. The inter-annual changes of sea-temperature anomaly in the western (solid line) and eastern (dashed line) Indian Ocean.

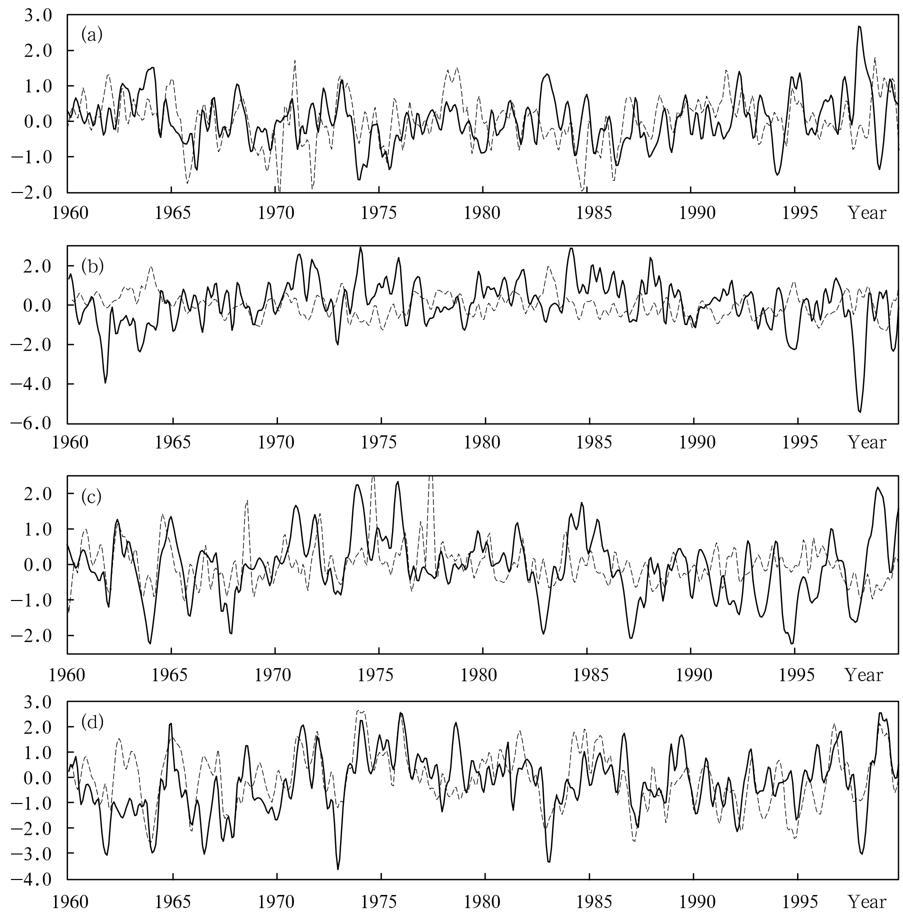

Fig.5. As in Fig.3, but for the Indian Ocean.

the changing MSTA depth is 0.23 and where the zonal wind (earlier by two months) and the temperature anomaly are of a positive correlation with a coefficient of 0.34 (see Fig.5d). Clearly, the Dipole event occurring in the Indian Ocean is an event of sea-air interaction as well.

5. The relations between the development of ENSO and Dipole

Saji et al. (1999) believed that the Dipole in the Indian Ocean was an event isolated from the Pacific ENSO. However, Webster et al. (1999) noted that the 1997/98 Indian Ocean sea-air interaction was an event associated with ENSO. Li and Mu (2001) argued that the Indian Ocean Dipole expressed by sea surface temperature anomaly was related to the Pacific ENSO. Having analyzed the relations between the subsurface sea-temperature anomalies of the two oceans and the zonal wind, Chao and Yuan (2003) concluded that Dipole and ENSO developed in a coordinated way. More data would be used as follows to demonstrate their relations.

Figure 6a shows the distribution of correlation coefficients of the equatorial eastern Pacific sea surface temperature and the sea temperature anomalies on the MSTA toroid of the two oceans at the same period, from which we can see that they are of an inverse correlation with the West Pacific warm pool sea temperature (a confidence of 99.9% and a correlation coefficient of 0.1), which is a El Niño pattern, while they are of an inverse correlation with the eastern Indian Ocean and a positive correlation with the western Indian ocean, the latter of which is a Dipole pattern. This indicates that the development of both El Niño and Dipole has much to do with the sea temperature anomaly on the ocean MSTA depth map. Figure 6b shows the correlation of the same period between the sea subsurface temperature in the above indicated western Indian Ocean zone and the sea temperature anomalies on the MSTA depth map of the two tropical oceans, from which it can be seen that it is of an inverse correlation with the eastern Indian Ocean sea

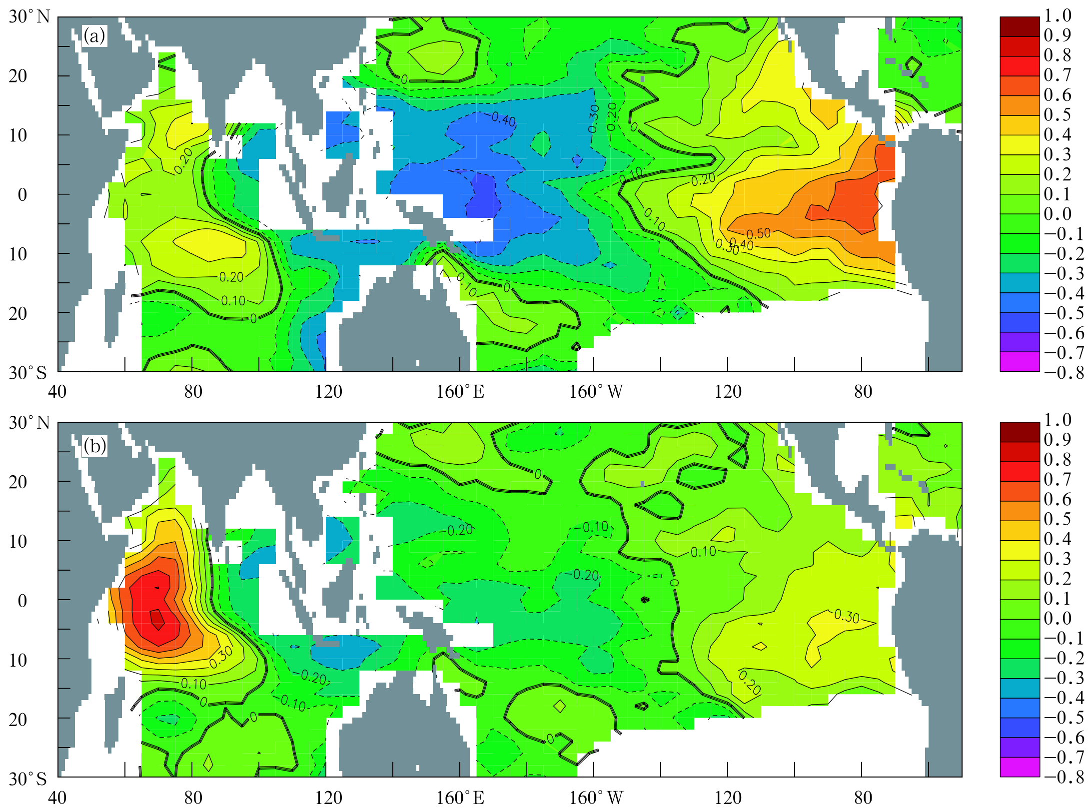

Fig.6. The correlation coefficient between subsurface sea-temperature anomaly and sea-temperature anomaly on the MSTA. (a) The eastern Pacific, and (b) the western Pacific.

temperature. This is an Indian Ocean Dipole, which is of an inverse correlation with the western Pacific sea temperature (the coefficient is over -0.2) and a positive correlation with the eastern Pacific one (the coefficient is over 0.2). This shows that from the statistical point of view (not any individual year), the development of both Dipole and El Niño features a strong correlation in terms of the sea temperature anomaly on the MSTA depth map.

As noted by Chao and Yuan (2003), the link between El Niño and Dipole is the pair of changing interdependent Walker circulations in the tropical Pacific and Indian Ocean, which shall be further analyzed here. The evolving Walker circulation can be expressed by a vertical movement calculated with the speed momentum that is associated with the wind convergence and divergence.

Figure 7 shows the distribution of correlation coefficients of the indicated western Indian Ocean zone sea temperature anomaly on the MSTA depth map and the speed momentum over the two tropical oceans. This distribution of correlation coefficient fields facilitates the deduction that when the western Indian Ocean subsurface temperature sees a positive (negative) anomaly, the central and western Indian Ocean experiences a rising (sinking) air current in the anomalous sense; the expanse from the central Indian Ocean to the central Pacific experiences a sinking (rising) air current; while the eastern Pacific experiences a rising (sinking) air current, thus blowing the anomalous easterly (westerly) wind in the low level from the western Pacific - eastern Indian Ocean to the western (eastern) Indian Ocean, and the anomalous westerly (easterly) wind from the western and central Pacific to the eastern (western) Pacific. This reflects the structure or pattern of the two zonal circulations (the so-called Walker circulation in the Pacific) cutting across the Indian and Pacific Oceans at a time when the western Indian Ocean sea subsurface temperature registers an anomaly.

Figure 8 shows the distribution of the correlation coefficients of the eastern Pacific sea temperature

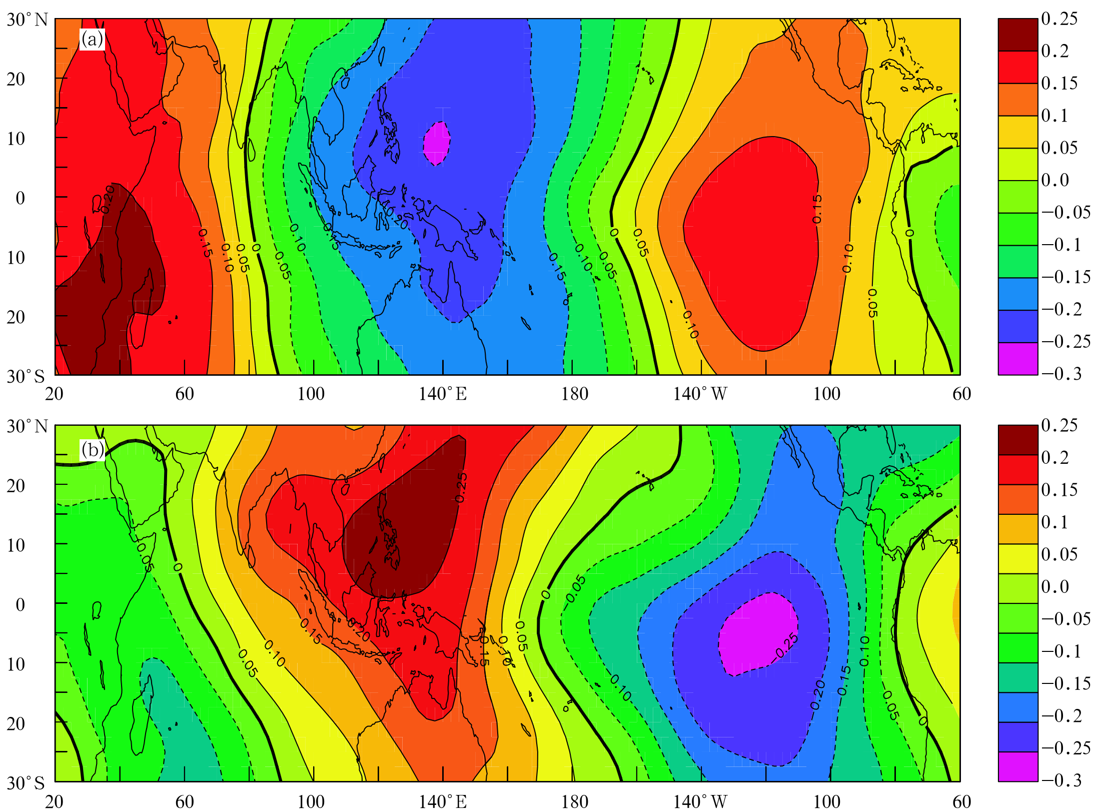

Fig.7. The correlation coefficient between sea-temperature anomaly on the MSTA in the western Indian Ocean and 200 hPa (a), 850 hPa (b) velocity potential.

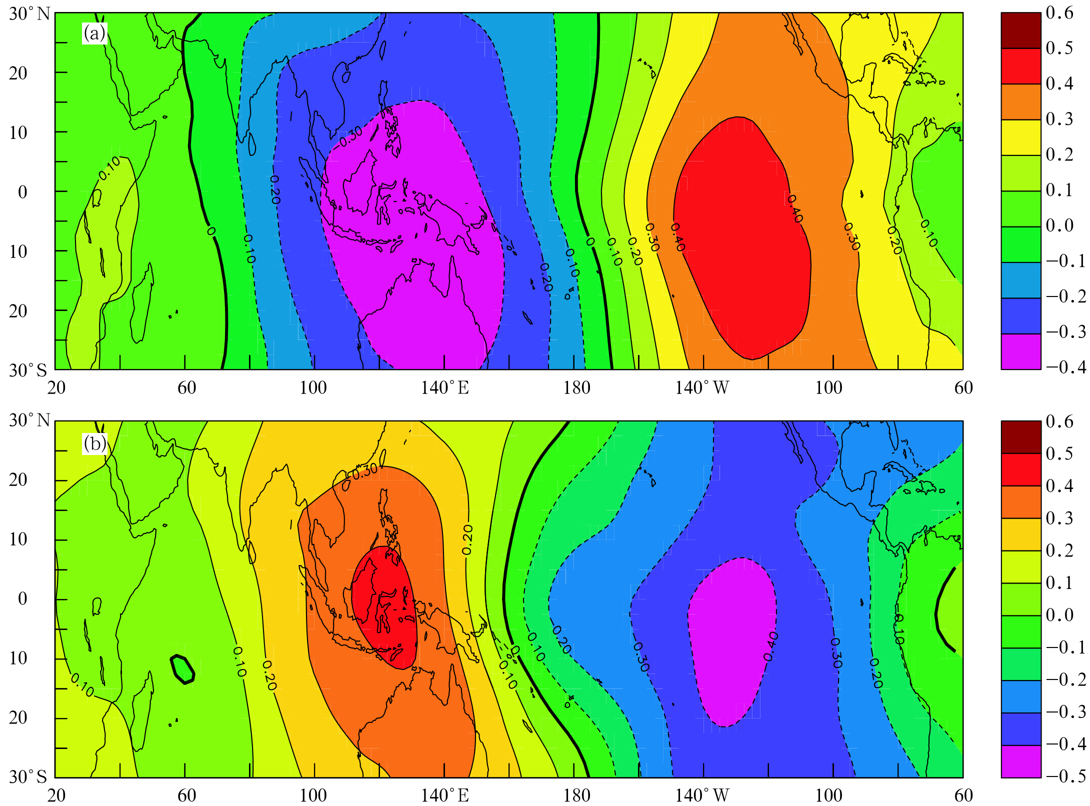

Fig.8. The correlation coefficient between sea-temperature anomaly on the MSTA in the eastern Pacific Ocean and 200 hPa (a), 850 hPa (b) velocity potential.

anomaly on the MSTA depth map and its speed momentum. Clearly, the distribution of correlation coefficient fields resembles that in Fig.7, hence the distributions of the rising and sinking air currents are alike.

These two figures reflect the sea-air interaction pattern in the Indian and the Pacific Oceans on the one hand and the development of such interaction on the other hand. In the statistical sense, the sea-air interaction events occurring in the two oceans are interrelated.

The above analysis of sea temperature anomaly and low zonal wind shows that the highest correlation coefficient goes to the earlier wind field sea temperature. Therefore, it can be concluded that the sea temperature anomalies of the two oceans are subject to the coupling of zonal circulations in the two tropical oceans.

6. Conclusion

Many recent data analyses indicate that the subsurface sea-temperature anomaly of the maximum depth map (a depth close to that of thermocline with 20°C as reference in the tropical Pacific) helps with the analysis of the development of El Niño and Dipole. The study shows that the Dipole events in the Indian Ocean are not isolated in most cases, but closely related to the development of ENSO instead. And the relationship between them is the Walker circulation that travels over the two oceans.

REFERENCES

Bjerknes, J., 1966: A possible response of the atmospheric Hadley circulation to equatorial anomalies of ocean temperature. *Tellus*, **18**, 820-829.

Bjerknes, J., 1969: Atmospheric teleconnection from the equatorial Pacific. *Mon. Wea. Rev.*, **97**, 163-172.

Chao Jiping and Yuan Shaoyu, 2003: Relationship of air-sea interaction in the tropical Pacific and Indian Ocean. *Progress in Natural Science*, **13**(12), 1280-1285. (in Chinese)

Chao Jiping, Yuan Shaoyu, and Cai Yi, 2003a: Large-scale air-sea interaction in the tropical Indian Ocean. *Acta Meteorologica Sinica*, **61**, 251-256. (in Chinese)

Chao Jiping, Yuan Shaoyu, Chao Qingchen, et al., 2003b: A data analysis study on the evolution of the El Niño/La Nina cycle. *Adv. Atmos. Sci.*, **19**, 837-844.

Chao Qingchen and Chao Jiping, 2001: The influence of western tropical Pacific and eastern Indian Ocean on the development of ENSO event. *Progress in Natural Science*, **11**(12), 1293-1300. (in Chinese)

Li Chongyin and Mu Mingquan, 1999: The occurrence of the El Niño event and the subsurface temperature anomaly of warm pool in the equatorial western Pacific. *J. Atmos. Sci.*, **23**, 513-526. (in Chinese)

Li Chongyin and Mu Mingquan, 2001: The Dipole in the equatorial Indian Ocean and its impacts on climate. *Chinese Journal of Atmospheric Sciences*, **25**, 433-443. (in Chinese)

Rasmusson, E. M., and T. H. Carpenter, 1982: Variation in tropical sea surface temperature and surface wind fields associated with the southern Oscillation/El Niño. *Mon. Wea. Rev.*, **110**, 354-384.

Saji, N. H., B. N. Goswami, P. N. Viayachandrom , et al., 1999: A dipole mode in the tropical Indian Ocean. *Nature*, **401**, 360-363.

Wang Zongshan, Zou Emei, J. M. Tool, L. J. Mangum, Xu Bochang, and Yang Kegi, 1990: *Air sea interaction in tropical Western Pacific*. Proc. US-PRC International TOGA Sym., Nov. 15-17, 1988, Beijing. Editor in Chief Chao Jiping and J. A. Young, Ed. China Ocean Press, 15-26.

Webster, P. T., A. M. Moore, J. P. Loschning, et al., 1999: Coupled ocean-atmosphere dynamics in the Indian ocean during 1997-98. *Nature*, **401**, 337-339.